5-8-2020

Observations on the Underlying Mechanisms Behind Particle-Melt Pool Interactions

Jonathon Azziz
Washington University in St. Louis

Katherine Flores
Washington University in St. Louis

Observations on the Underlying Mechanisms Behind Particle-Melt Pool Interactions

Jonathon Azziz[1]& Katharine Flores[1,2]

1. Department of Mechanical Engineering & Materials Science, Washington University; St Louis, MO
2. Institute of Materials Science & Engineering, Washington University; St Louis, MO

Abstract

Additive manufacturing processes are key to changing the manufacturing landscape for years to come. Despite this however, these processes are not entirely understood. One such process, the LENS system, and its incorporation mechanisms of metal particles into a melt pool are incredibly complex. Therefore, an investigation of those mechanism was undertaken as a way to understand and improve the LENS additive manufacturing process. High-speed videos made it possible to observe the interactions between particles and the melt pool. The interactions were categorized in order to find trends that presented themselves throughout the data. Multiple correlations were drawn between surface tension characteristics, incorporation speeds, particle size, particle behavior, particle location, and the timing of each event. From these correlations, it is possible to conclude that surface tension plays a large role in the incorporation mechanism, but other mitigating factors, such as oxide layers or additional particle heating should not be discounted. It is also likely that particle incorporation time is heavily dependent upon particle location, particle size, and the timing of the event with respect to the overall process.

1 Introduction

Ever since they were first introduced in the early seventies, additive manufacturing processes have always been denoted as the wave of the future. There are, of course, a multitude of types and sub-types of additive manufacturing, but metallic additive manufacturing, or metal 3D printing, is one of the primary sets of processes key to reimagining the future of manufacturing. Despite these procedures being so key for the future, however, they are still not entirely understood. The purpose of the research discussed here is to illuminate the underlying mechanisms of metal 3D printing, while the conclusions drawn from the data will help us to better utilize the process in the future.

1.1 History

While additive manufacturing first came about in the late seventies, they were all polymer and plastic based, thus making them ill advised for industrial uses. It was not until nearly two decades later that metal additive manufacturing techniques were first being discovered. The first patent for a metal additive manufacturing was DMLS (direct metal laser sintering) and it was filed in the 1990s by the Fraunhofer Institute in

Germany (Meiners, 1996). Ever since then, engineers, researchers, and scientists have come up with other methods for printing with metal, some of which are entirely unique and some that are just different enough from DMLS to be awarded their own patents. Even now, some forty-odd years later, metal additive manufacturing processes are not entirely refined and are often more experimental than not.

1.2 Metal Powder Bed Fusion (PBF)

This category of additive manufacturing includes Direct Metal Laser Sintering (DMLS), Selective Laser Melting (SLM) and Electron Beam Melting (EBM) as its three most common processes. DMLS and SLM are similar in theory as they are both additive manufacturing techniques designed to use a high power-density laser to melt and fuse metallic powders together (Xometry, 2020). However, each technique is slightly different. The primary difference between the two is the difference between melting and sintering. Sintering uses a combination of heat and pressure to make particles stick together. Melting uses high enough temperatures to cause the particles to fully melt and join together. Sintered parts have high porosity and require heat treatments to be strengthened, though they will never be as strong as forged metal parts; melted parts are nearly fully solid and don't require post-process heat treatments. Consequently, SLM processes work with a single metal at a time, while DMLS works with metal alloys. The EBM process is very similar to DMLS with the exception of an electron beam in place of the high power-density laser.

1.3 Direct Energy Deposition

Direct Energy Deposition (DED), Direct Metal Deposition (DMD) or Laser Engineered Net Shaping (LENS) processes are a second set of additive manufacturing techniques commonly found in industry today and are the focus of the research covered in the aforementioned experiments. In powder-fed directed-energy deposition, a high-power laser is used to melt metal powder supplied to the focus of the laser beam. Metal powder is delivered and distributed around the circumference of the head or can be split by an internal manifold and delivered through nozzles arranged in various configurations around the deposition head. A hermetically sealed chamber filled with inert gas or a local inert shroud gas is often used to shield the melt pool from atmospheric oxygen for better control of material properties. The powder fed directed energy process is similar to the SLS process, but the metal powder is applied only where material is being added to the part at that moment. The process supports a wide range of materials including titanium, stainless steel, aluminum, and other specialty materials as well as composites and functionally graded material (Thre3d, 2014).

Throughout the course of these experiments, the LENS process has been recorded and studied so that a better understanding of the incorporation mechanisms between the metal powder particles and the laser melt pool could be gained and hopefully lead to an increase in the overall process efficiency.

2 Methodology

2.1 LENS Setup and Materials

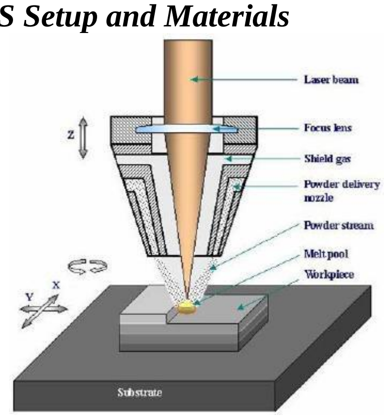

Figure 1. Primary setup of the LENS system (Chang, 2013)

For the experiments, the setup visualized above in Fig. 1 was used. A continuous high-power laser ranging from 150-300 W output power and a constant processing speed was used. Powder particles were applied using a coaxial nozzle at transport gas flow rates ranging from 4.5-8.5 l/min and powder feed rates ranging from 1.12-2.12 rpm. Argon was used as transport and shielding gas. Both the powder and substrate materials were Ti-64Al-4V (Ti64) titanium alloy. Powder size distribution of the chosen powder was from 50 to 150 µm. A highspeed camera (Photron Fastcam mini AX 200) with a long distance 3-12x microscope lens were positioned to observe the particle interaction with the melt pool. The process itself consisted of depositing a single track 12 mm in length and then doubling back such that 10 mm of the track was a two layers high and the remaining 2 mm was only a single layer high.

2.2 High-Speed Imaging

Video sequences were evaluated to derive the powder particle behavior when interacting with the melt pool surface (Fig. 2). The outline of the melt pool was identified in the highspeed videos by determining the moving surface transition to the solid material. Particle behaviors were defined based on the observation of the interactions between the powder particles and the melt pool. The time of each event was measured with respect to the overall length of each video and thus is marked by video frames and later converted to seconds. Only particles that incorporated into the melt pool were considered.

3 Results

3.1 Observed Particle Behaviors

Particle interactions with the melt pool and the following described behaviors were all observed via the high-speed images taken during the track deposition. As seen below in Table 1 and Figure 2, there are twelve behaviors overall, grouped 1-12 in order of frequency of occurrence. For example, the most observed behavior became 1, the second most observed became 2, etc. After initial observations, two groups, seen below as 6 and 11, were added as behavioral subsets of groups 5 and 8, respectively.

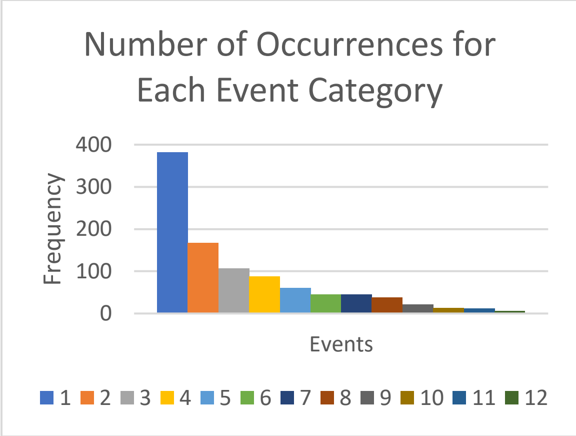

Figure 2. Histogram of Event Frequency

Ranking of Occurrence	Behavior
1	Lands on the edge of the melt pool and slowly incorporates into the pool
2	Crashes through the liquid surface of the melt pool and lands on the bottom of the pool, causes a ripple effect, and is “swallowed” by the ripples’ return
3	Penetration of the liquid surface with no other behavior
4	Lands in the center of the melt pool, and incorporates slowly
5	Misses the melt pool, but “pops” and incorporates into the melt pool
6	Misses the melt pool, and slowly incorporates into the pool
7	Collides with the melt pool, rests for a few frames on the surface and then sinks rapidly
8	Lands on the path before the melt pool and is eventually incorporated
9	Lands on the path before the melt pool and “pops”
10	Lands on the edge of the melt pool and subsequently does not incorporate, but gets left behind as the melt pool moves on
11	Lands on the surface of the melt pool and instead of incorporating immediately, the particle skates around the surface before exhibiting behavior seen in Group B
12	The 1st particle lands on the edge of the melt pool and begins to slowly incorporate. A 2nd particle lands on top of the 1st, which stops melting, and then the combined mass of the two particles “tip over” into the pool.

Table 1. Particle-melt pool behaviors organized by frequency of occurrence

3.2 Observed Particle Characteristics

Along with each particle’s incorporative behavior, their inherent characteristics were observed and recorded as well. Those characteristics, more specifically diameter and time of impact, were then plotted with respect to their individual categories in order to identify correlations in between the multiple data sets. To test whether the diameter data was able to be approximated as normal, a sample of the Ti-64 powder was placed in the Scanning Electron Microscope (SEM), see Figure 3 above, and the diameters of each particle were recorded.

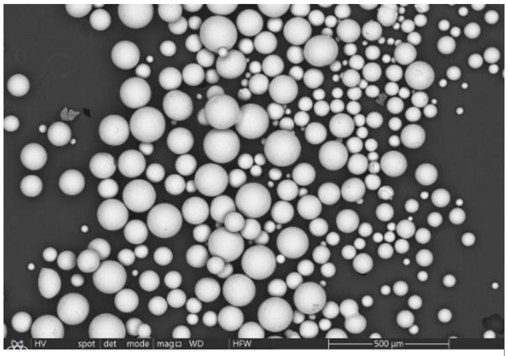

Figure 3. SEM image of a Ti-64 powder sample

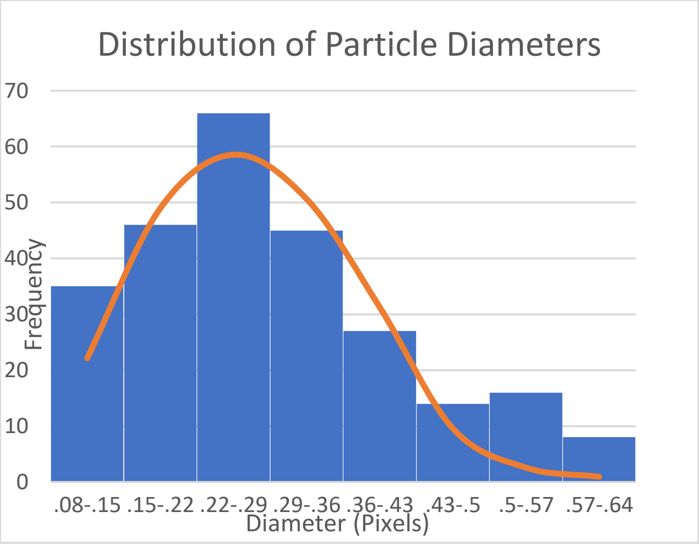

Figure 4. The distribution of particle diameters for the entire data set. While not perfect, the data can be approximated as normal

A second set of test data with the same mean and standard deviation as the diameter set was randomly generated. As seen above, in Figure 4, the distribution of particle sizes can be approximated as normal, thus allowing for the data analysis performed later on in the experiments. Figures 5 and 6 below illustrate the average time of impact and average particle diameter for each of the aforementioned event categories.

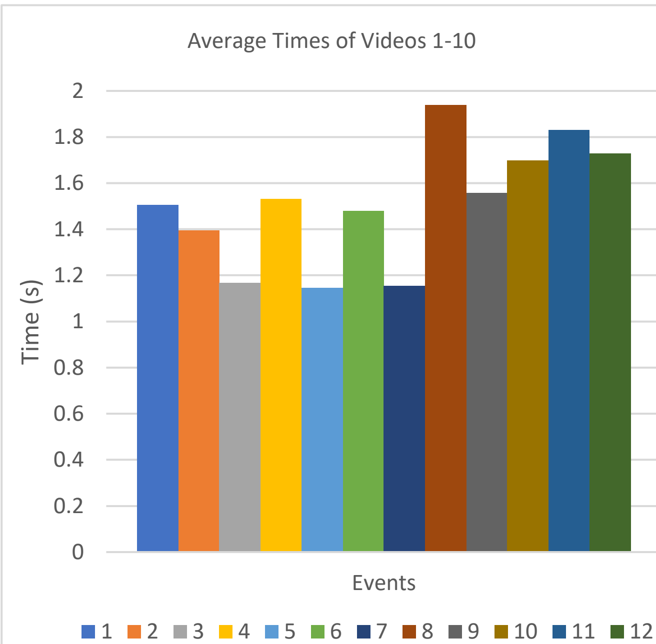

Figure 5. The average time of impact of each event category

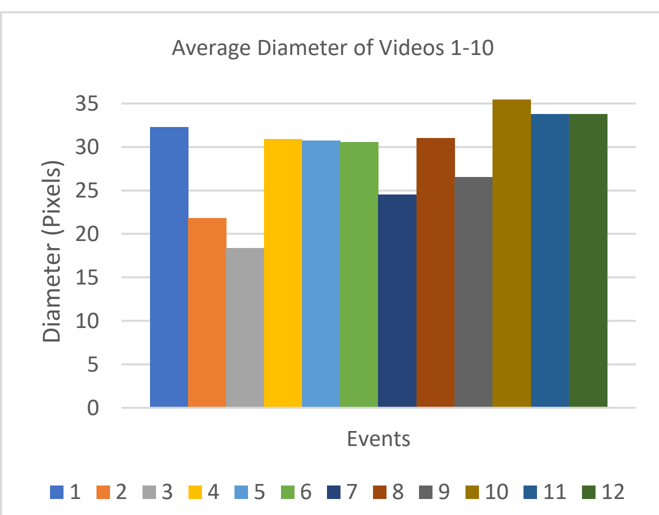

Figure 6. The average diameter of the Ti-64 particles

4 Discussion

4.1 Surface Tension Characteristics

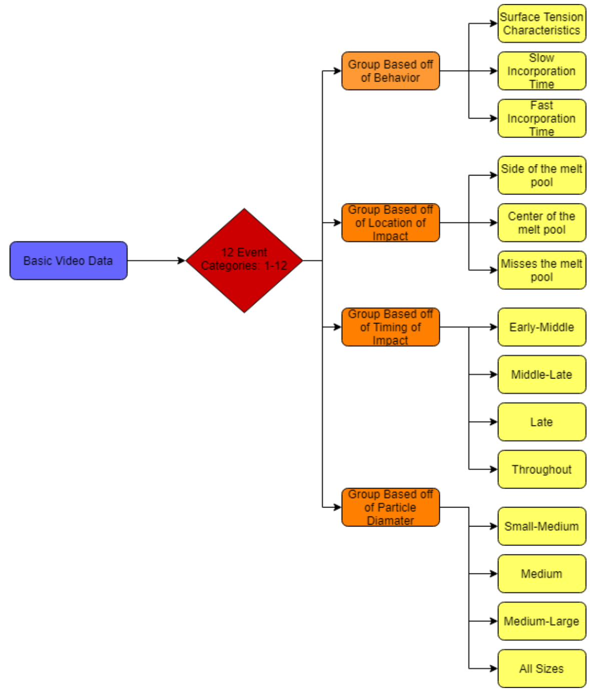

Figure 7. Flowchart detailing the narrowing down process from basic event categories to more defined groups

After the data collection was finished, and the event categories defined, the next step was of course, to find possible trends and patterns. As seen above in Figure 7, the twelve initial groups were narrowed down into sets based off of four primary descriptors: Location of Impact, Timing of Impact, Particle Diameter, and overall behavior. This last set is the primary focus of the data analysis. The behavior set was then split into 3 groups, with each group displaying a shared characteristic. The three groups were as follows: Slow incorporation times, fast incorporation times, and surface tension characteristics. The remaining data from the original twelve groups did not fit into any shared category and thus were excluded from the following analyses. Table 2 below shows which event types make up each of the subgroups, seen in yellow in the flow chart.

Groups	Event Types
Surface Tension Characteristics	2,7,9
Slow Incorporation Time	1,4,6,8
Fast Incorporation Time	5,11
Side of the Melt pool	1,8,10,11
Center of the Melt pool	2,3,4,7
Misses the Melt pool	5,6,12
Early-Middle	7
Middle-Late	4,5,6,8
Late	9,11,12
Throughout	1,2,3,10
Small-Medium	3
Medium	2,7,8
Medium-Large	1,4,5,11,12
All Sizes	6,9,10

Table 2. Behavioral subgroups (left) and the event types that comprise them (right)

By looking at the surface tension behavior group, a rough sense of the surface tension characteristics displayed during the LENS process can be gained. The data is made of what was originally groups 2, 7, and 9 (See Table 1 for reference). The capillary action present in the ripples of event type 2 suggest a high amount of surface tension present in the liquid melt pool. The brief lack of incorporation seen in events 7 and 9 appears to suggest the same. But what does this really say about the surface tension during the LENS process?

4.1.1 Temperature Dependence

As seen in Figure 5 above, the previously mentioned surface tension data sets, 2, 7, and 9, all occur roughly in the middle time range in the video. Conversely, surface tension characteristics do not appear in either the early time ranges of the video where the overall temperature should be higher. This would suggest that higher temperatures correspond with lower surface tension, and thus would hypothesize that surface tension is not only temperature dependent, but inversely related to temperature.

4.1.2 Particulate Size Dependence

As seen above in Figure 6, the surface tension data sets, 2, 7, and 9, all occur in the mid-range for particle diameters. One can conversely infer that surface tension characteristics do not appear in either the small or large range particle diameters. There are a number of reasons why surface tension does not appear in the extreme particle diameter ranges, but it most likely caused by a difference in forces. As all of the particles are moving when they impact on the surface of the liquid, one can hypothesize that the kinetic energy of the particles is larger than the opposing surface tensions and thus breaks the surface without any observable surface tension characteristics. The kinetic energy of the particles can be attributed in two ways. The smaller particles have less mass and thus a higher velocity which will increase the overall kinetic energy. The larger particles have less velocity, but more mass, again increasing the kinetic energy and canceling out the surface tension.

4.2 Incorporation Time Behavior

As a reminder, after narrowing down the initial twelve event groups, the behavior set was then split into 3 groups, with each group displaying a shared characteristic. The three groups were as follows: Slow incorporation times, fast incorporation times, and surface tension characteristics.

By looking at the both incorporation time groups, a rough sense of the efficiency of the LENS process can be gained. The data for the slow incorporation time group is made of what was originally groups 1, 4, 6, and 8 (See Table 1 for reference). The data for the fast incorporation time group is made of what was originally groups 5 and 11. As incorporation time increases, the overall time to create a part increases as well. If the overall time to create a part can be decreased without sacrificing the quality of the part, then the efficiency of the process can increase. By studying the specific groups that increase and decrease incorporation time, the behaviors which increase and decrease efficiency can be observed and possibly put into effect in later processes.

4.2.1 Particle Size Dependence

As seen above in Figure 6, the slower incorporation time sets, 1, 4, 6, and 8, occur in the larger particle size range. This would suggest that the larger a particle's diameter, the longer it takes to incorporate. A possible cause for this would be that larger particle diameters corresponds to more material, thus more material to melt, which increases the incorporation time.

In terms of the overall efficiency of the LENS system, the possible particle size dependence would be seen as a careful balancing act. If the hypothesis is true, then larger particles decrease the efficiency of the system. However, if the particles carry more material, they will add more material to the part, thus effectively reducing the number of particles needed. Conversely, while small particles may speed up incorporation time, they add less material and thus require more particles to complete the part.

4.2.2 Temperature Dependence

As seen in Figure 4 above, the previously mentioned slow incorporation data sets, 1, 4, 6, and 8 occur near the middle of the video. This could suggest that mid-range temperatures correspond with slower incorporation times. Conversely, by looking at the fast incorporation groups, 5 and 11, which occur at earlier and later times respectively, we can surmise that higher and lower temperatures increase incorporation times. These trends would suggest that incorporation time is temperature dependent.

With respect to the efficiency of the system, the possible temperature dependence would again, be a careful balancing act. While the previously discussed arguments with respect to increasing and decreasing incorporation time still stand, increasing and decreasing temperature bring their own arguments. Increasing temperature would increase the power used by the system, thus making it less energy efficient. Decreasing the temperature while keeping the laser power constant, depending on the method, may also increase the power used by the system and again reducing efficiency.

4.2.3 Event Location Dependence

By cross referencing the event types found in the Behavior and Location subsets, see Table 2, a correlation between slow incorporation times and location was discovered. After collecting all of the shared data into a new set, it was found that slower incorporation times occurs at the sides of the melt pool. It could be theorized that the location dependent incorporation time is a result of a relative temperature difference. The non-liquid substrate, just outside the edge of the melt pool has a lower relative temperature than the liquid melt pool, hence it is not melted. When a particle is ejected via the gas nozzles, it often passes through the laser while still in midair. Passing through the laser could momentarily heat up the particle such that when it lands on the non-melted substrate it has a higher relative temperature than the substrate. The substrate produces a cooling effect on the particle and thus it takes longer to heat the particle up to its melting temperature. The increase in heating times directly increases the incorporation times.

In terms of system efficiency, the efficiency could be increased if the gas nozzle direction were adjusted so that it more accurately aimed for the melt pool. Similar results would be gained if the nozzle were adjusted to produce a narrower spray of particles, which be more precise, and if aimed correctly, more accurate.

4.3 Future Work

As of now, all of the preceding hypotheses are untested in both the realms of this experiment and Ti-64. That being said, future experiments will be required to test these hypotheses empirically. More specifically data on the overall process temperature over time, the mass and velocity of individual sample particles, the temperature of individual sample particles, and finally the temperature of the substrate just outside of the liquid melt pool will all be needed to prove or disprove these hypotheses.

The underlying mechanisms of particle-melt pool interactions were investigated via the observations of particle-melt pool collisions. Due to both the lack of empirical data and the theoretical nature of the observations outlined previously, only hypotheses were able to be produced as results. That being said, the hypotheses seem to be in good standing, covering all of the trends in support of them and seemingly lacking any logical fallacies.

However, the hypotheses are not all encompassing. While the hypotheses were all rooted in either particle behavior, diameter, location of impact, or time of impact, those are not the only causes for discrepancies in overall behavior. What I believe to be the primary causes for concern are possible oxide layers covering the particles and lack of uniform density throughout the particles, i.e., partial hollowing out or pitting. The oxide layer would compensate for anomalies regarding the incorporation times as the presence of an oxide would likely increase the incorporation time. The lack of uniform density would also account for discrepancies found in incorporation time data. A lack of uniform density would also account for a number of other single event behavioral anomalies as well. These anomalies were observed only a handful of times at most and were so bizarre, that they were largely left out of the analyses outlined above. Examples include floating or bouncing particles, instantaneous “popping” effects; different than those described in event types 5 and 11, particles that were liquid before they reach the surface, etc.... A floating particle could be explained by nonuniform density, if, after the outer shell of a hollow particle was melted, gasses trapped inside were freed and launched the particle into the air. Similarly, popping particles could simply be hollowed out and have far less material to melt, thus making their incorporation faster than the average particle. Once again however, these are hypotheses that will require future experiments to either confirm or deny.

5 Conclusions

The analysis of particle-melt pool behaviors, experimentally measured physical particle characteristics, as well as the timing and location of impact events reveals correlations dotting back and forth among them. It can be hypothesized that both surface tension and incorporation times are temperature dependent and that incorporation times are reliant upon impact location and particle diameters.

By analyzing incorporation times, a sense of the overall LENS process efficiency can be understood. Lower incorporation times theoretically means an increase in efficiency and vise vera.

However, the act of improving efficiency has always been a double-edged sword. Increase efficiency in one area and decrease it in another. Such is the case here as one tries to cite the incorporation times as a possible area for improvement. Decrease particle size, decrease incorporation time, but increase the number of particles needed to finish the job. Similar arguments present themselves when looking at temperature and location dependent incorporation times.

Future experiments, specifically producing plots of temperature over time, particle velocity and mass data, density uniformity data, and many others will be needed for these hypotheses to be useful in a practical environment.

6 Acknowledgments

We are very thankful for the work done by Dr. Patricia Weisensee and the members of her lab, Sean Lopez and Tharun Reddy, in providing the high-speed videos used as the basis for this experiment. We are also very grateful to the Institute of Materials Science & Engineering (IMSE) for allowing access to their scanning electron microscope (SEM). Finally, we would like to acknowledge the other members of Dr. Flores' lab group, Mu Li and Porter Weeks for their assistance with various parts of the experiment.

References

1. ASTM F2792 - 12a Standard Terminology for Additive Manufacturing Technologies, (Withdrawn 2015)". Astm.org. Retrieved 2017-04-26.
2. "DMLS | Direct Metal Laser Sintering | What Is DMLS?". Atlantic Precision.
3. Beese, Allison M.; Carroll, Beth E. (2015-12-21). "Review of Mechanical Properties of Ti-6Al-4V Made by Laser-Based Additive Manufacturing Using Powder Feedstock". JOM. 68 (3): 724–734.
4. Chang, Kuang-Hua. (2013). Rapid Prototyping. 10.1016/B978-0-12-401745-0.00005-8.
5. Cheng, B., Loeber, L., Willeck, H. et al. Computational Investigation of Melt Pool Process Dynamics and Pore Formation in Laser Powder Bed Fusion. J. of Materi Eng and Perform 28, 6565–6578 (2019). https://doi.org/10.1007/s11665-019-04435-y
6. Paul K. Chu; XinPei Lu (15 July 2013). Low Temperature Plasma Technology: Methods and Applications. CRC Press. p. 455. ISBN 978-1-4665-0991-7.
7. Gibson, Ian; Rosen, David; Stucker, Brent (2015). "Chapter 10". Additive Manufacturing Technologies - Springer. doi:10.1007/978-1-4939-2113-3. ISBN 978-1-4939-2112-6.
8. Hideo Kodama, "Automatic method for fabricating a three-dimensional plastic model with photo-hardening polymer," Review of Scientific Instruments, Vol. 52, No. 11, pp. 1770–73, November 1981
9. "Shaped body especially prototype or replacement part production", issued 1996-12-02
10. "Metal 3D Printing: An Overview Of The Most Common Types - 3D Printing." 3D Printing. N. p., 2019. Web. 30 Apr. 2020.
11. Prinz, F. B.; Merz, R.; Weiss, Lee (1997). Ikawa, N. (ed.). Building Parts You Could Not Build Before. Proceedings of the 8th International Conference on Production Engineering. London, UK: Chapman & Hall. pp. 40–44.
12. "How Laser Powder Forming Works". THRE3D.com.
13. Volpp, J. Behavior of powder particles on melt pool surfaces. Int J Adv Manuf Technol 102, 2201–2210 (2019). https://doi.org/10.1007/s00170-018-03261-1
14. "Direct Metal Laser Sintering". Xometry.